

Supporting Information

pH- and glutathione-responsive release of curcumin from mesoporous silica nanoparticles coated using tannic acid-Fe(III) complex

Sanghoon Kim,^{a,b*} Stéphanie Philippot,^{a,c,d} Stéphane Fontanay,^{a,c,d} Raphaël E. Duval,^{a,c,d}
Emmanuel Lamouroux,^{a,b} Nadia Canilho,^{a,b} and Andreea Pasc^{a,b*}

^a CNRS, UMR 7565, SRSMC, F-54506 Vandoeuvre-les-Nancy, France

^b Université de Lorraine, UMR 7565, SRSMC, Faculté des Sciences et Technologies, F-54001 Vandoeuvre-les-Nancy, France

^c Université de Lorraine, UMR 7565, SRSMC, Faculté de Pharmacie, F-54001 Nancy, France

^d ABC Platform®, F-54001 Nancy, France

* Corresponding authors. Tel.: +33 3 83 68 46 61 (AP)

Email address: sanghoon.kim@univ-lorraine.fr (SK), andreea.pasc@univ-lorraine.fr (AP)

1. FT-IR spectra of multilayer coated MSN

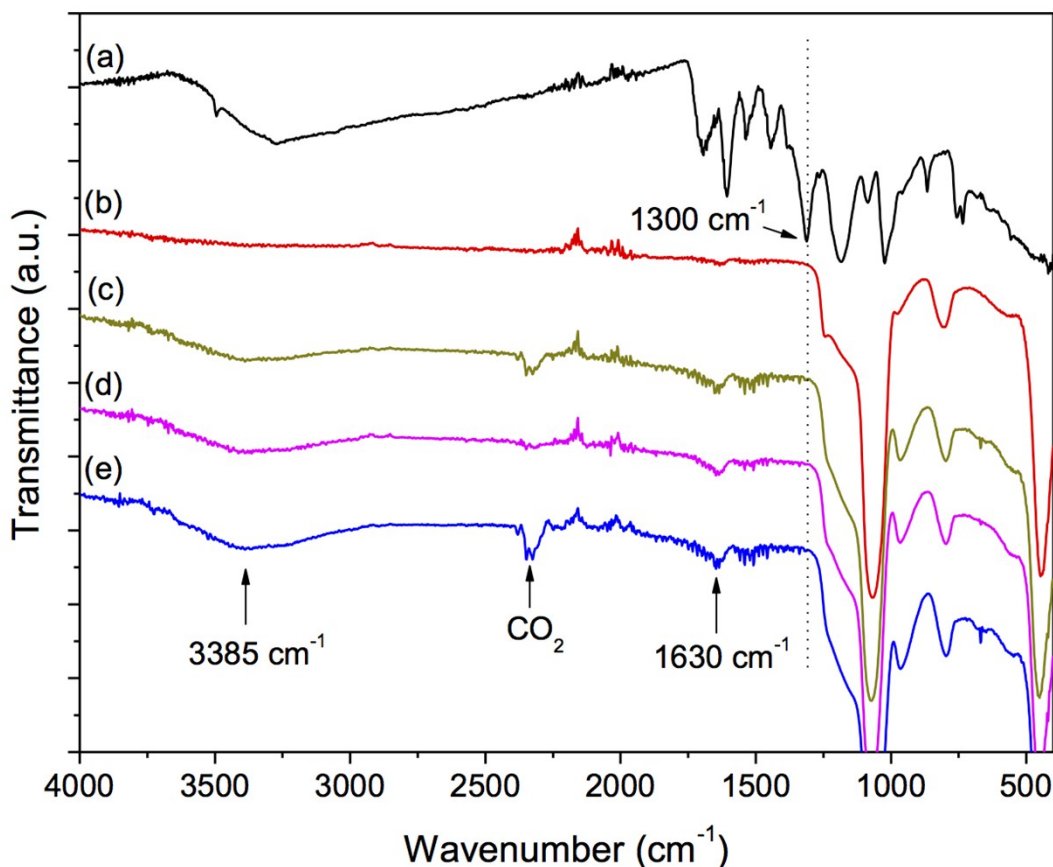


Fig. S1. FT-IR spectra of (a) tannic acid, (b) MCM-41, (c) MCM-41-TA (coated 1 time), (d) MCM-41-TA-2 (coated 2 times) and (e) MCM-41-TA-3 (coated 3 times). All spectra were normalized based on Si-O-Si stretching (1080 cm⁻¹)

As shown in Fig. S1, a characteristic band for free (non bonded to Fe) OH stretching of tannic acid (3385 cm⁻¹) and C=O stretching band (1630 cm⁻¹) became more pronounced as multilayers of tannic acid-Fe(III) were formed (Fig. S1-c to e). In this study, curcumin loaded MCM-41 materials were not tested, because OH stretching band and C=O stretching band of curcumin could overlap with OH stretching of tannic acid. Moreover, after TA-Fe(III) coating process, the weakness of intensity for aromatic C-OH stretching peaks of tannic acid (1300 cm⁻¹ to 1020 cm⁻¹) was also observed, and especially for the peak at 1300 cm⁻¹, the reduce of the intensity was dramatic, which could be interpreted as TA-Fe(III) complex formation.(ref. 40 of the manuscript)

2. Additional SEM data for MCM-41-CU-TA

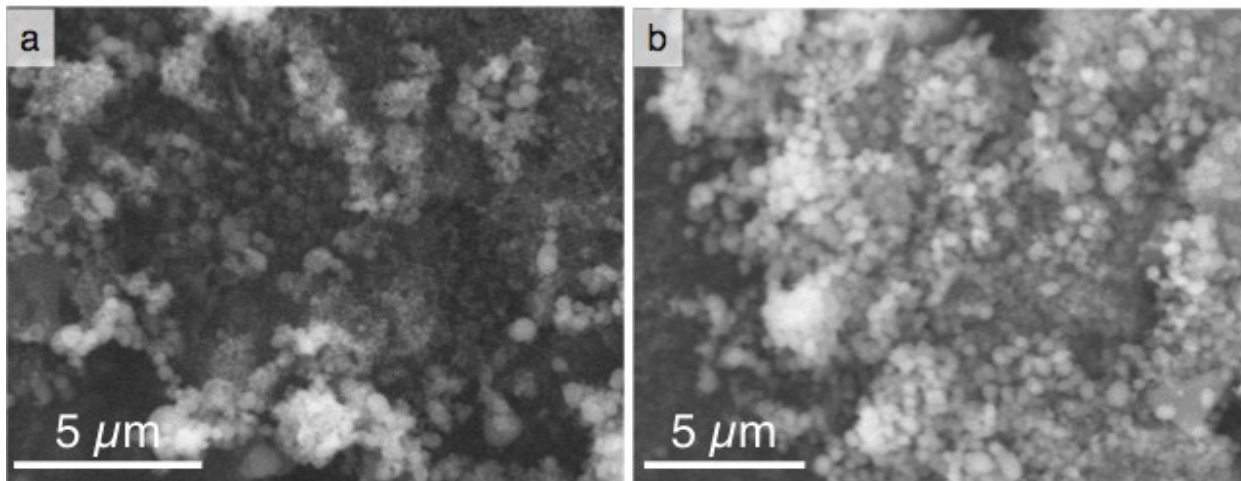


Fig. S2. SEM image of (a) MCM-41, (b) MCM-41-CU-TA

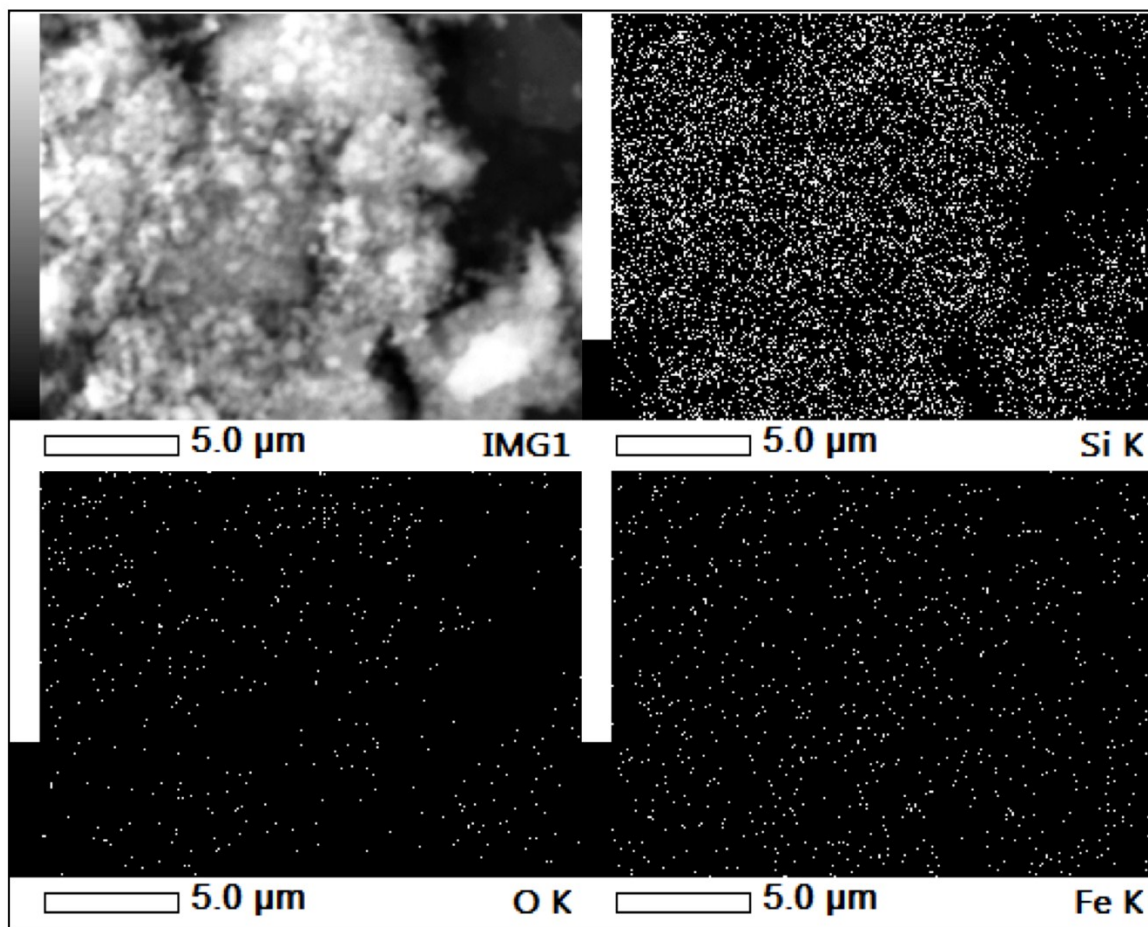


Fig. S3. SEM-EDS mapping image of MCM-41-CU-TA

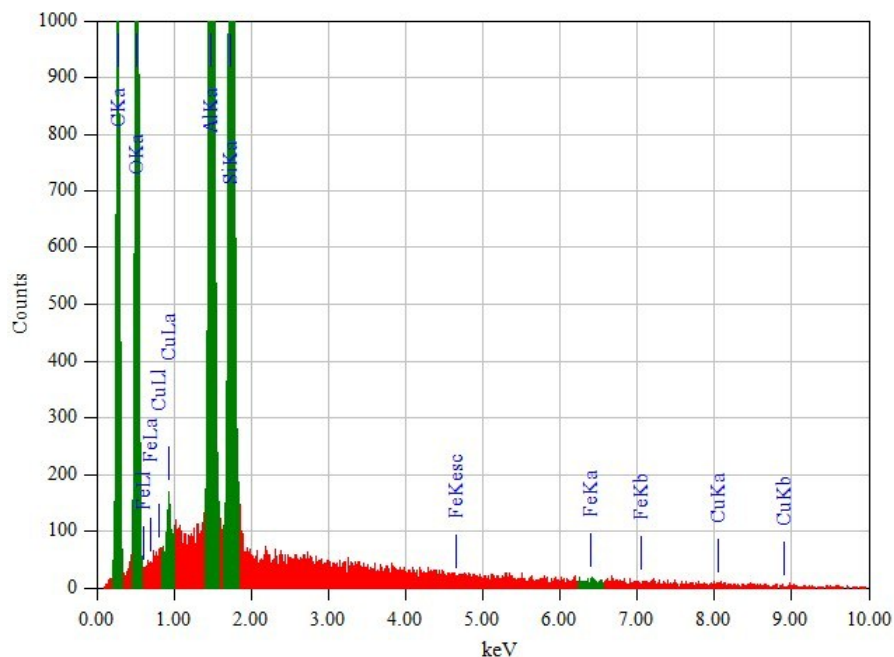


Fig. S4. SEM-EDS elemental analysis of MCM-41-CU-TA

Element	KeV	Mass%	Atom%
O (K)	0.525	67.47	78.50
Si (K)	1.739	32.34	21.43
Fe (K)	6.398	0.19	0.06

Table S1. SEM-EDS elemental analysis of MCM-41-CU-TA

3. Calculation of tannic acid-Fe(III) complex in the mesoporous silica nanoparticles.

For 4 mg of silica material after coating process, the amount of tannic acid was calculated as following: $24 \text{ mol/L} * 0.02 \text{ mL} * 1701 \text{ g/mol} * 0.125 * 1\text{L}/1000\text{mL} = 0.102 \text{ mg}$, where 24mol/L is the concentration of tannic acid in stock solution, 0.02 mL for the volume used, 1701 g/mol is molar weight of tannic acid, and 0.125 is the ratio of tannic acid-Fe(III) charge transfer band peak before/after coating process, determined by UV-vis spectroscopy. (Fig. S5)

The amount of Fe(III) can be also described in the same manner: $24 \text{ mol/L} * 0.02 * \text{mL} * 55.8 \text{ g/mol} * 0.33 * 0.125 * 1\text{L}/1000\text{mL} = 0.001 \text{ mg}$ of Fe(III) ion, where 55.8 g/mol is molar weight of Fe, 0.33 is the ratio between tannic acid and Fe(III) in the complex. The possibility of Fe (III) ions coordinated to other functional groups was neglected in the calculation.

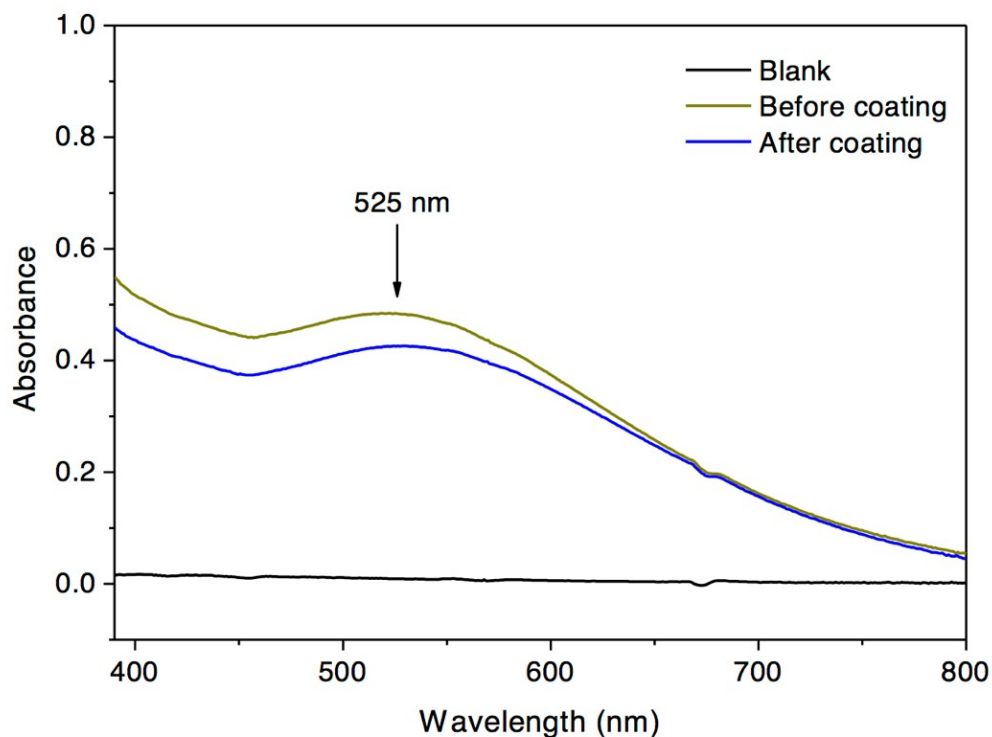


Fig. S5. UV spectra of tannic acid-Fe(III) complex before/after coating process.

4. Calculation of curcumin content in the mesoporous silica nanoparticles.

10 mg of tannic acid-Fe(III) coated curcumin loaded mesoporous silica nanoparticles, MCM-41-TA-CU was added to 5 mL of 0.1M HCl solution for the decomposition of tannic acid-Fe(III) complex. Then, 95 mL of THF was added to extract and solubilize curcumin. The solution was analysed using UV-vis spectroscopy. The calculated curcumin content was 8.2 wt.%. (93 % with respect to initially loaded amount)

5. Additional TEM images

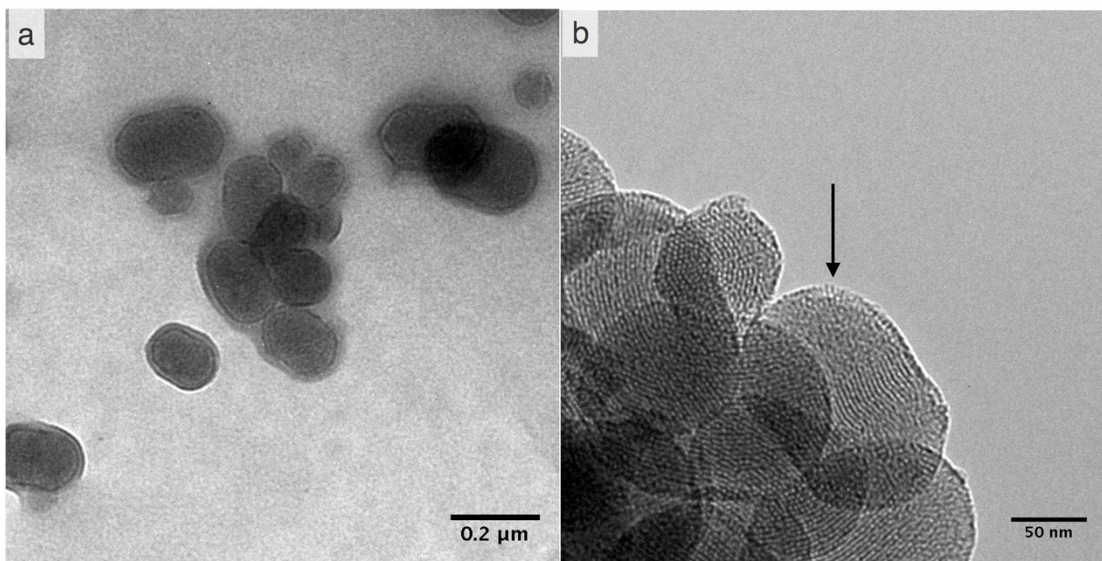


Fig. S6. TEM image of (a) MCM-41-CU-TA, (b) MCM-41-CU-TA-3 incubated at 2.5, arrow indicates opened mesopores.

6. Characterization of SBA-15 silica materials.

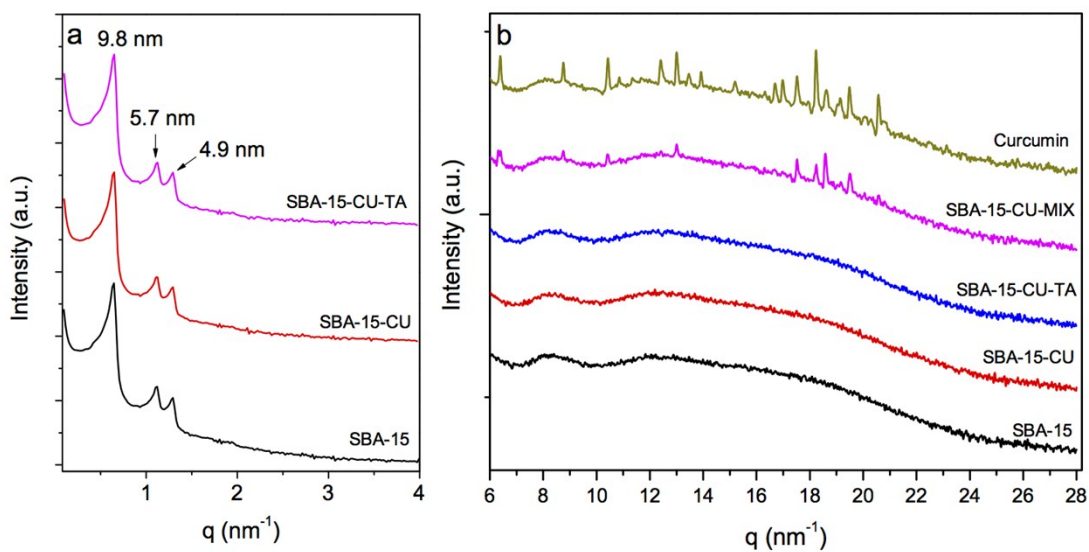


Fig. S7. (a) SAXS patterns of SBA-15 with and without curcumin loading, and before and after surface coating, (b) WAXS patterns of SBA-15 mesoporous materials with and without

curcumin loading, before and after surface coating, and of physical mixtures of curcumin with SBA-15.

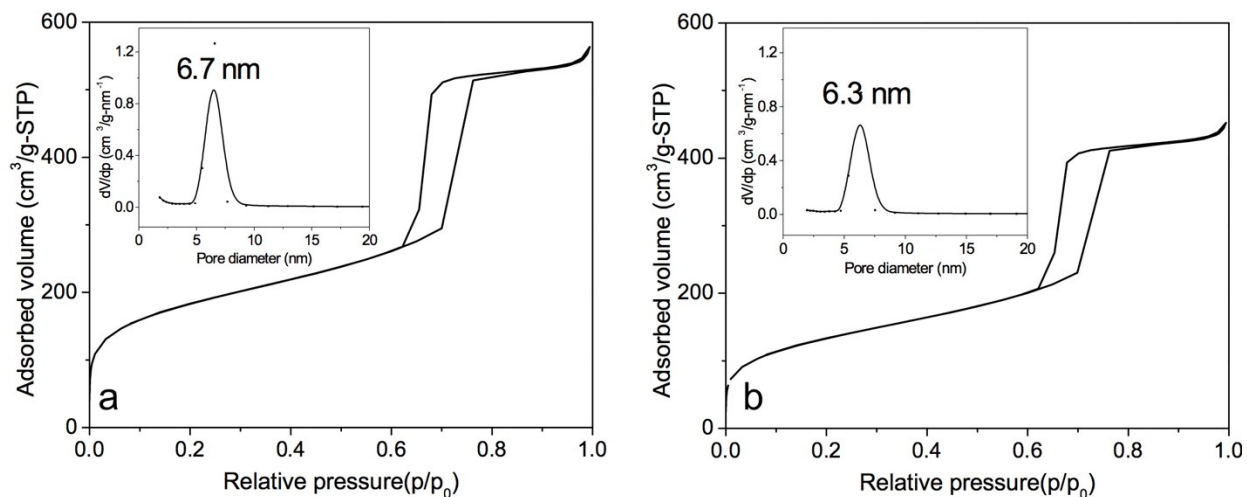


Fig. S8. N₂ adsorption–desorption isotherms and pore size distribution (inset) of (a) SBA-15, (b) SBA-15-CU.

The BET specific surface area and the mesopore volume are 638 m² g⁻¹ and 0.91 cm³ g⁻¹ for (a) SBA-15, 461 m² g⁻¹ and 0.70 cm³ g⁻¹ for (b) SBA-15-CU, respectively

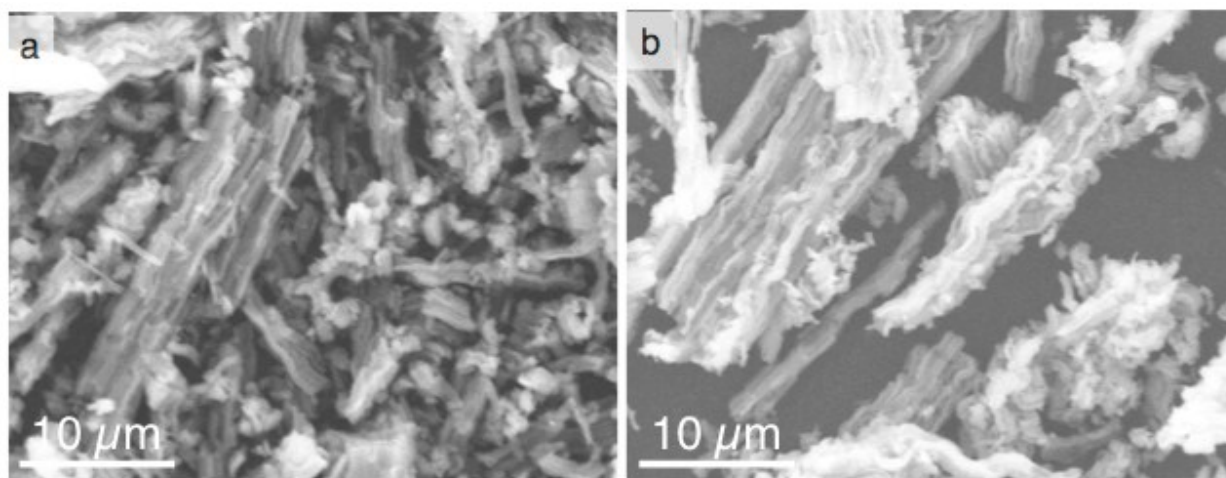


Fig. S9. SEM image of (a) SBA-15, (b) SBA-15-CU-TA

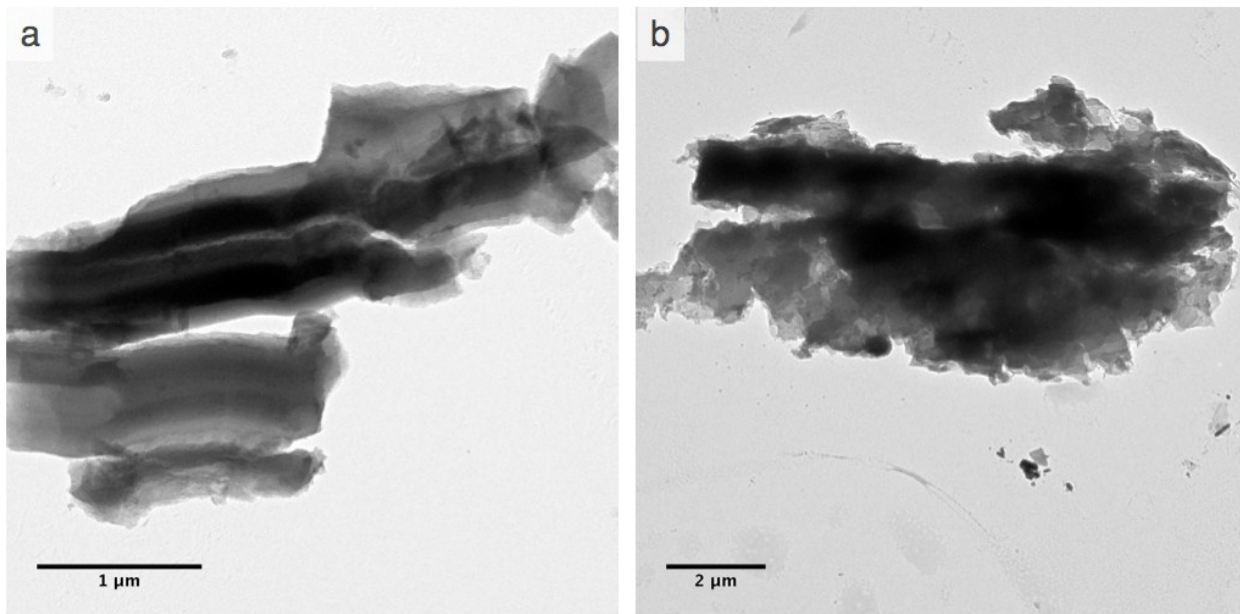


Fig. S10. TEM image of (a) SBA-15, (b) SBA-15-CU-TA